G0/G1 switch gene-2 regulates human adipocyte lipolysis by affecting activity and localization of adipose triglyceride lipase

Martina Schweiger,* Margret Paar,* Christina Eder,* Janina Brandis,* Elena Moser,* Gregor Gorkiewicz,† Susanne Grond,* Franz P. W. Radner,* Ines Cerk,* Irina Cornaciu,* Monika Oberer,* Sander Kersten,§ Rudolf Zechner,* Robert Zimmermann,[1,]* and Achim Lass[1,]*

Institute of Molecular Biosciences* University of Graz, 8010 Graz, Austria; Institute of Pathology,† Medical University of Graz, 8036 Graz, Austria; and Nutrition, Metabolism, and Genomics Group,§ Wageningen University, 6700 EV Wageningen, The Netherlands

Abstract The hydrolysis of triglycerides in adipocytes, termed lipolysis, provides free fatty acids as energy fuel. Murine lipolysis largely depends on the activity of adipose triglyceride lipase (ATGL), which is regulated by two proteins annotated as comparative gene identification-58 (CGI-58) and G0/G1 switch gene-2 (G0S2). CGI-58 activates and G0S2 inhibits ATGL activity. In contrast to mice, the functional role of G0S2 in human adipocyte lipolysis is poorly characterized. Here we show that overexpression or silencing of G0S2 in human SGBS adipocytes decreases and increases lipolysis, respectively. Human G0S2 is upregulated during adipocyte differentiation and inhibits ATGL activity in a dose-dependent manner. Interestingly, C-terminally truncated ATGL mutants, which fail to localize to lipid droplets, translocate to the lipid droplet upon coexpression with G0S2, suggesting that G0S2 anchors ATGL to lipid droplets independent of ATGL's C-terminal lipid binding domain. Taken together, our results indicate that G0S2 also regulates human lipolysis by affecting enzyme activity and intracellular localization of ATGL. Increased lipolysis is known to contribute to the pathogenesis of insulin resistance, and G0S2 expression has been shown to be reduced in poorly controlled type 2 diabetic patients. Our data indicate that downregulation of G0S2 in adipose tissue could represent one of the underlying causes leading to increased lipolysis in the insulin-resistant state.— Schweiger, M., M. Paar, C. Eder, J. Brandis, E. Moser, G. Gorkiewicz, S. Grond, F. P. W. Radner, I. Cerk, I. Cornaciu, M. Oberer, S. Kersten, R. Zechner, R. Zimmermann, and A. Lass. **G0/G1 switch gene-2 regulates human adipocyte lipolysis by affecting activity and localization of adipose triglyceride lipase. *J. Lipid Res.* 2012.** 53: **2307–2317.**

Supplementary key words comparative gene identification-58 • human lipolysis • regulation • insulin resistance

In periods of nutrient scarcity or in response to increased energy demand, triglyceride (TG) stores are mobilized to provide free fatty acids (FFAs) as energy fuel. The mobilization of TGs is performed in three consecutive reactions, catalyzed by three lipases: adipose triglyceride lipase (ATGL) (1–3), hormone-sensitive lipase (HSL) (4), and monoglyceride lipase (MGL) (5). The crucial physiological role of ATGL (also annotated as patatin-like phospholipase domain containing 2, desnutrin, phospholipase A2ζ, and transport secretion protein 2.2) in lipolysis became evident by the phenotype of ATGL-deficient (ATGL-ko) mice. ATGL-ko mice display increased whole-body fat mass, enlarged adipose fat depots, and TG accumulation in many tissues. Massive TG deposition in cardiomyocytes leads to cardiac insufficiency and premature death (6). In humans, the lack of ATGL activity, caused by mutations in the ATGL gene, is associated with a rare inherited disorder, annotated as neutral lipid storage disease with myopathy (NLSDM) (7). This disease is characterized by TG deposition in multiple tissues and cardiac myopathy.

ATGL activity is strongly influenced by regulatory proteins. In 2006, Lass et al. identified comparative gene identification-58 (CGI-58, also known as ABHD5) as coactivator of

This work was supported by the "GOLD: Genomic of Lipid-associated Disorders" grant, which is part of the Austrian Genome Project "GEN-AU: Genome Research in Austria" funded by the Austrian Ministry for Science and Research and the FFG. This work was also supported by grants P21296, F30-SFB-LIPOTOX, Doktoratskolleg W901, and Wittgenstein Award Z136, which are funded by the Austrian Science Foundation. Additional funding was obtained from the City of Graz and the Province of Styria.

Manuscript received 13 April 2012 and in revised form 19 July 2012.

Published, JLR Papers in Press, August 13 2012
DOI 10.1194/jlr.M027409

Abbreviations: ATGL, adipose triglyceride lipase, CGI-58, comparative gene identification-58; CV, column volume; DG, diacylglycerol; G0S2, G0/G1 switch gene-2; hMADS, human adipose-derived stem cell; hMSC, human mesenchymal stem cell; HSL, hormone-sensitive lipase, LacZ, β-galactosidase; LD, lipid droplet; MGL, monoglyceride lipase; MOI, multiplicity of infection; NLSDM, neutral lipid storage disease with myopathy; PKA, protein kinase A; PPAR, peroxisome proliferator-activated receptor; SGBS, Simpson-Golabi-Behmel syndrome; TCEP, tris(2-carboxyethyl)phosphine; TG, triglyceride; WAT, white adipose tissue.

[1] To whom correspondence should be addressed.
e-mail: achim.lass@uni-graz.at (A.L.); robert.zimmermann@uni-graz.at (R.Z.)

ATGL, which is required for efficient lipolysis (8). Newborn mice lacking CGI-58 exhibit increased fat mass and die a few hours after birth, most likely due to a severe skin defect (9). Similarly, mutations in the CGI-58 gene in humans have been associated with a rare disease characterized by systemic TG accumulation and defective skin function, annotated as NLSD with ichthyosis (NLSDI) or Chanarin-Dorfman syndrome (10). Although CGI-58 is essential for ATGL activation, observations in humans and mice suggest that CGI-58 possesses an additional function in lipid metabolism that is independent of ATGL and specifically important in skin. Independent groups reported that the protein exhibits acyl-CoA-dependent lysophosphatidic acid acyltransferase activity (11, 12). To date, the significance of this activity in the development of the severe skin defect in mice lacking CGI-58 or in patients suffering NLSDI is unclear.

More recently, Yang et al. identified G0/G1 switch gene-2 (G0S2) as an inhibitory protein of ATGL (13). This protein was initially identified in 1991 to be transiently expressed in lymphocytes during the switch from the G0 to the G1 phase of the cell cycle (14). A very recent study reported that G0S2 interacts with nucleolin, resulting in its cytosolic retention and thereby leading to reduced proliferation of hematopoetic stem cells (15). The role of G0S2 in the cell cycle remains unknown, but the protein was shown to be involved in apoptosis (16). Recent evidence suggests that G0S2 acts as antipode of CGI-58, specifically inhibiting ATGL activity (13). G0S2 expression is downregulated in response to fasting and increased upon refeeding in humans and chickens (17, 18). Accordingly, the antilipolytic hormone insulin increases G0S2 expression in murine 3T3 cells, whereas stimulation of lipolysis by β-adrenergic agonists and tumor necrosis factor-α has the opposite effect (13, 19). Importantly, a recent report demonstrated that G0S2 mRNA and protein expression is reduced in adipose tissue of type 2 diabetic humans, indicating that enhanced ATGL activity contributes to elevated lipolysis and plasma fatty acid (FA) levels in type 2 diabetes (20).

At present, the role of G0S2 in human adipocyte lipolysis has not been studied. The aim of our study was to investigate how G0S2 is involved in the control of human adipocyte lipolysis. Our data suggest that G0S2 efficiently inhibits human ATGL activity and promotes the binding of the enzyme to lipid droplets (LDs).

RESEARCH DESIGN AND METHODS

Human tissue samples

All human tissues were collected from autopsies and snap frozen. The study has been approved by the ethics committee of the Medical University of Graz, Austria, according to local regulations.

Animals

Mice (C57Bl/6) were maintained on a regular light-dark cycle (12 h light, 12 h dark) and kept on a standard laboratory chow diet (4.5% w/w fat). For tissue collection, ad libidum-fed mice were euthanized by cervical dislocation, then the tissues were excised and snap frozen. Maintenance, handling, and tissue collection from mice has been approved by the Austrian Federal Ministry for Science and Research and by the ethics committee of the University of Graz.

cDNA cloning of recombinant proteins

Human ATGL (hATGL), murine ATGL (mATGL), human CGI-58 (hCGI-58), and murine CGI-58 (mCGI-58) were cloned as described (21). Sequences containing the complete open reading frame of hATGL, human G0S2 (hG0S2), and murine G0S2 (mG0S2) were amplified by PCR from human and murine cDNAs using Phusion Polymerase (Finnzymes, Thermo Scientific, Finland). cDNA was prepared from mRNA using SuperScript Reverse Transcriptase protocol (Life Technologies, Carlsbad, CA). The primers were designed to create Kozak initiation sequence (*italic*) and restriction endonuclease cleavage sites (underlined) for subsequent cloning strategies: hG0S2forw 5′CCAGGATCCGAAACGGTCCAGGAGCTG3′, hG0S2rev 5′CCGCTCGAGCTAGGAGGCGTGCTGC 3′, mG0S2forw 5′GGAATTCGAAAGTGTGCAGGAGCTGATCCC3′, mG0S2rev 5′GCTCGAGTTAAGAGGCGTGCTGCCGGA3′, hATGLYFPforw 5′ATCTCGAG*ccaccatg*TTTCCCCGCGAGAAGACG3′, hATGLYFPrev 5′GTGGATCCCGCAGCCCCAGGGCCCCGATCA3′, mG0S2CFPforw 5′GGAATTCG*ccaccatgg*AAAGTGTGCAGGA3′, and mG0S2CFPrev 5′GGGTACCGTAGAGGCGTGCTGCCGCA3′.

PCR products were ligated to compatible restriction sites of the eukaryotic expression vector pcDNA4/HisMaxC (Life Technologies), pECFP-N1, or pEYFP-C1 (BD Biosciences, Palo Alto, CA).

Generation of hATGL mutants by site-directed mutagenesis

Mutations in *hATGL* (FS282 = h319X, h289X) were introduced at the positions of the ATGL coding sequences as described (21).

Sequence analysis

Sequence analyses of plasmid DNA were performed using BigDye terminator kit (Applied Biosystems, Foster City, CA) and an ABI PRISM 310 Genetic analyzer (Applied Biosystems).

Cloning and amplification of adenovirus encoding mG0S2, shRNA for hATGL, and siRNA for hG0S2

For the generation of recombinant adenovirus expressing mG0S2 (AdG0S2), the following primers were used to amplify murine G0S2 from the mouse cDNA-containing plasmid and to be flanked with XhoI and *Hin*dIII restriction endonuclease sites (underlined) for oriented ligation: AdG0S2 fw: 5′ CCGCTCGAGTTAGCGCAGAGGCTTGGG 3′ and Ad G0S2 rv: 5′TAAGCTTTAGAGTATAAAAGGTTTTTATTTCAAAATGC 3′.

For the generation of shRNA specific for hATGL, the following primers were designed to amplify the coding sequence from bp 202 to bp 222 and to be flanked with BamHI and *Hin*dIII restriction endonuclease sites (underlined) for oriented ligation:

ATGL shRNA fw: 5′GGATCCGTTCATTGAGGTATCTAAATTCAAGAGATTTAGATACCTCAATGAACTTA3′, and ATGL shRNA rv: 3′GCAAGTAACTCCATAGATTTAAGTTCTCTAAATCTATGGAGTTACTTGAATTCGA5′.

Primers were annealed and ligated with the pSilencer 4.1-CMV purovector according to the manufacturer's protocol (Ambion, Austin, TX). Silencing capacity of cloned shRNA constructs was determined by cotransfection with an expression vector encoding hATGL in Cos-7 cells. The G0S2 PCR product or the ATGL shRNA was cloned into the pShuttle vector (pAd Easy XL Adenoviral Vector system, Stratagene, Santa Clara, CA) and transformed into *E. coli* BJ5183-AD-1 (which contains the pAdEasy-Vector) for recombination. Recombinant Ad plasmid was isolated, verified by restriction analysis, and transfected into HEK-293 cells using the calcium-phosphate method (Stratagene) for virus production. Virus particles were isolated using CsCl gradient banding (22). Predesigned MISSION siRNA for human G0S2 was obtained from Sigma-Aldrich (St. Louis, MO). siRNA starting at position

281 bp of the G0S2 gene: (5′CCAAGGAGAUGAUGGCCCA3′) as well as MISSION siRNA Universal Negative Control #1 (Sigma-Aldrich) were used for silencing experiments.

Expression of recombinant proteins and preparation of cell lysates

Monkey embryonic kidney cells (Cos-7; ATCC CRL-1651) were cultivated in DMEM (GIBCO, Invitrogen, Carlsbad, CA), containing 10% fetal calf serum (FCS; Sigma-Aldrich) and antibiotics (100 IU/ml penicillin and 100 µg/ml streptomycin) at standard conditions (37°C, 5% CO_2, 95% humidified atmosphere). Cells were transfected with 1 µg DNA complexed to Metafectene (Biontex, Munich, Germany) in serum free DMEM. After 4 h, the medium was replaced by DMEM supplemented with 10% FCS. For the preparation of cell lysates, cells were washed with 1× PBS, collected using a cell scraper, and disrupted in buffer A (0.25 M sucrose, 1 mM EDTA, 1 mM dithiothreitol, 20 µg/ml leupeptine, 2 µg/ml antipain, 1 µg/ml pepstatin, pH 7.0) by sonication (Virsonic 475; Virtis, Gardiner, NJ). Nuclei and unbroken cells were removed by centrifugation (1,000 *g*, 4°C, for 10 min). Determination of protein concentrations of cell lysates and detection of His-tagged proteins by Western blotting analysis were performed as described below.

Preparation of tissue homogenates and extracts

Human and murine tissue samples were washed in PBS containing 1 mM EDTA and homogenized on ice in buffer A using an Ultra Turrax (IKA, Staufen, Germany). Homogenates were centrifuged for 30 min at 20,000 *g* and 4°C to obtain tissue extracts. Protein content was determined as described below.

Purification of human recombinant G0S2

Human G0S2 was subcloned into a modified pET28b(+)vector, transformed into *E. coli* BL21(DE3) CodonPlus (Stratagene, La Jolla, CA) cells, and expressed during exponential growth for 3 h at 30°C. The original pET-28b(+) vector (Novagen, Merck Biosciences, Darmstadt, Germany) was modified by introducing an N-terminal yeast small ubiquitin-like modifier (Smt) fusion protein and a TEV protease cleavage site between the Smt fusion and the multiple cloning site of the vector [pET28b(+)-TEV-Smt]. Cells were harvested and resuspended in buffer B [50 mM Tris-HCl, pH 7.5, 500 mM NaCl, 10% glycerol, 20 mM imidazole, 1 mM benzamidine, 1 mM tris(2-carboxyethyl)phosphine TCEP], and lysed by sonication (SONOPLUS ultrasonic homogenizer, Bandelin, Berlin, Germany). After centrifugation (20,000 *g*, 4°C, 30 min) the His-tagged hG0S2 was separated by affinity chromatography using a preequilibrated Ni-column (GE Healthcare, Waukesha, WI). Proteins were eluted in 10 column volumes (CV) of 0–100% buffer C (as buffer B but containing 500 mM imidazole) gradient followed by 10 CVs 100% buffer C. Fractions containing hG0S2 were dialyzed against 50 mM Tris-HCl, pH 7.5, 300 mM NaCl, 10% glycerol, 1 mM EDTA, and 1 mM TCEP. After overnight TEV-protease cleavage at 4°C of the Smt tag, the untagged hG0S2 was isolated under denaturing conditions (6M urea) using a preequilibrated Ni-column by collecting the flow through. The proteins were refolded via dialysis against 50 mM Tris-HCl, pH 7.5, 300 mM NaCl, 10% glycerol, 1 mM EDTA, and 1 mM TCEP and further purified on a size exclusion column (Superdex 200, GE Healthcare, Pittsburgh, PA).

Immunoblotting

Western blotting analysis was performed with lysates of Cos-7 (20 µg), Simpson-Golabi-Behmel syndrome (SGBS), and 3T3-L1 cells (75 µg) or mouse and human tissues (50 µg). Proteins were separated by SDS-PAGE and blotted onto a PVDF membrane (Carl Roth, Karlsruhe, Germany). His-tagged proteins were detected using a mouse anti-His antibody (GE Healthcare, Buckinghamshire, UK). ATGL was detected using a commercial rabbit anti-ATGL polyclonal antibody (Cell Signaling Technology, Boston, MA). CGI-58 was detected using a rabbit anti-CGI-58 antiserum kindly provided by Dr. Dawn L. Brasaemle (Rutgers Center for Lipid Research and Department of Nutritional Sciences, New Brunswick, NJ). For G0S2 detection, a combined human/mouse polyclonal antibody directed against epitopes TVLGGRALSNRQHAS and EATLCSRALSLRQHAS of the human and mouse G0S2 proteins, respectively, were generated in rabbit and peptide affinity-purified (Eurogentec, Maastricht, The Netherlands). Primary antibodies were detected using horseradish peroxidase-conjugated anti-rabbit (Vector Laboratories, Burlingame, CA) or anti-mouse (GE Healthcare) IgG antibody and visualized by enhanced chemiluminescence detection (ECL; GE Healthcare).

Determination of TG hydrolase activity

For the determination of TG hydrolase activity of cell lysates containing various recombinant proteins or tissue extracts, samples in a total volume of 100 µl buffer A were incubated with 100 µl substrate in a water bath at 37°C for 60 min. TG substrate was prepared by emulsifying 330 µM triolein (40,000 cpm/nmol) and 45 µM phosphatidylcholine/phosphatidylinositol (3:1) in 100 mM potassium phosphate buffer (pH 7.0) by sonication and adjusted to 5% essentially FA-free BSA. As a control, incubations under identical conditions were performed in buffer A alone. After incubation, the reaction was terminated by adding 3.25 ml of methanol/chloroform/heptane (10:9:7) and 1 ml of 0.1 M potassium carbonate and 0.1 M boric acid (pH 10.5). After centrifugation (800 *g*, 15 min), the radioactivity in 1 ml of the upper phase was determined by liquid scintillation counting. Counts from control incubations were subtracted and the rate of FA hydrolysis was calculated using ^3H radiolabeling of triolein substrate.

Cultivation and differentiation of SGBS cells

SGBS preadipocytes were provided by Novo Department of Pediatrics and Adolescent Medicine, University of Ulm, Germany. Cells were maintained in DMEM/Nutrient Mix F12 (GIBCO, 1/1, v/v), supplemented with 8 µg/ml biotin (Sigma-Aldrich), 4 µg/ml pantothenic acid (Sigma-Aldrich), 10% FCS, 100 IU/ml penicillin, and 100 µg/ml streptomycin at 37°C in 5% CO_2, 95% humidified atmosphere. For differentiation, SGBS cells were seeded at 30,000 cells/well in 6-well plates. Seven days after seeding, differentiation was induced using the differentiation medium 1 [DMEM/Nutrient Mix F12 1/1, v/v, 100 IU/ml penicillin, 100 µg/ml streptomycin, 8 µg/ml biotin, 4 µg/ml pantothenic acid, 0.01 mg/ml transferrin (Sigma-Aldrich), 1 µM cortisol (Sigma-Aldrich), 200 pM triiodothyronine (Sigma-Aldrich), 20 nM human insulin (Sigma-Aldrich), 0.25 µM dexamethasone (Sigma-Aldrich), 500 µM 3-isobutyl-1-methylxanthine (Sigma-Aldrich), and 2 µM rosiglitazone (Axxora, San Diego, CA)]. On day 4 of differentiation, the medium was replaced by differentiation medium 1. On days 8 and 11 of differentiation, the medium was replaced by differentiation medium 2 (DMEM/Nutrient Mix F12 supplemented with 100 IU/ml penicillin, 100 µg/ml streptomycin, 8 µg/ml biotin, 4 µg/ml pantothenic acid, 0.01 mg/ml transferrin, 1 µM cortisol, 200 pM triiodotyronine, 20 nM human insulin, in the presence or absence of 1 µM rosiglitazone). SGBS cells were fully differentiated on day 14.

Infection and electroporation of SGBS cells

On day 10 of differentiation, SGBS cells were infected with 1,000, 800, and 600 multiplicity of infection (MOI) of adenoviruses encoding murine G0S2 or β-galactosidase (LacZ) as control, respectively. For silencing ATGL expression, cells were infected with 600 and 800 MOI of adenoviruses encoding shRNA specific for ATGL or

β-galactosidase (LacZ) as control, respectively. Cells were used for experiments two days postinfection (i.e., on day 12). On day 8 of differentiation, 100 pmol siRNA specific for G0S2 or negative control siRNA per 10^6 cells were electroporated into SGBS cells using Neon Transfection System (Life Technologies) with a pulse of 1,400 V for 20 ms. Then cells were seeded in poly-D-lysine (Millipore) coated 12-well plates at a density of 300,000 cells/well and grown in respective differentiation medium 1 or 2 but lacking antibiotics. The next day, medium was replaced by differentiation medium 2 containing antibiotics. Cells were used for experiments four days postelectroporation (i.e., on day 12).

Measurement of lipolysis of SGBS adipocytes and analysis of reaction products

Differentiated SGBS adipocytes were conditioned in DMEM/Nutrient Mix F12, containing 2% essentially FA-free BSA in the absence or presence of 25 μM of the HSL-specific inhibitor NNC 0076-0000-0079 (kindly provided by Novo Nordisk, Copenhagen, Denmark) for 60 min. Thereafter, the medium was replaced by an identical, fresh medium and lipolysis was stimulated by addition of 10 μM forskolin (Sigma-Aldrich). As control, DMSO was added. After 120 min of incubation, aliquots of the medium were removed and analyzed for FFA content using commercial kits (Wako Chemicals, Neuss, Germany; Sigma). To determine intracellular TG levels, total lipids were extracted with hexane/isopropanol (3/2) and dried under nitrogen. Thereafter, lipids were dissolved in 1% Triton X-100 and TG concentration was measured using a commercial kit (Thermo Electron, Thebarton, Australia).

In another set of experiments, differentiated SGBS cells were electroporated with siRNAs specific for hG0S2 or control siRNA, cultured for three days, and loaded with 0.4 mM oleic acid (complexed to essentially FA-free BSA and containing 4 mCi ^{3}H-9, 10-oleate/mmol as tracer, 1 μCi per 6-well). The next day, cells were washed with PBS, containing 2% essentially FA-free BSA and incubated for 1 h in DMEM/Nutrient Mix F12 containing 2% essentially FA-free BSA. Radioactivity in the supernatant was determined by liquid scintillation counting (Tri-Carb 2300 TR, Packard). For protein determinations, cells were washed three times with PBS and lysed in 0.3 N NaOH/0.1% SDS. For the analysis of lipolytic reaction products, cellular lipids were extracted three times with hexane/isopropanol (3/2) and evaporated. After the addition of 10 μg/ml tri-, di- (*sn*-1,2 and *sn*-2,3) and monoolein (Sigma-Aldrich) as internal standards, lipids were dissolved in chloroform and separated by TLC (TLC silica plates 60, Merck, Darmstadt, Germany) using chloroform/acetone/acetic acid (96/4/1) as solvent. Bands corresponding to diolein were excised and radioactivity was determined by liquid scintillation counting.

Cultivation and differentiation of 3T3-L1 cells

3T3-L1 fibroblasts (CL-173) were obtained from ATCC (Teddington, UK) and cultivated in DMEM containing 4.5 g/l glucose and L-glutamine (Invitrogen) supplemented with 10% FCS and antibiotics under standard conditions (37°C, humidified atmosphere, 5% CO_2). Two days after confluence, medium was changed to DMEM supplemented with 10% FCS containing 10 μg/ml insulin (Sigma-Aldrich), 0.25 μM dexamethasone (Sigma-Aldrich), and 500 μM isobutylmethylxanthine (Sigma-Aldrich) in the presence or absence of 1 μM rosiglitazone (Axxora). After three and five days, medium was changed to DMEM supplemented with 10% FCS containing 10 μg/ml and 0.05 μg/ml insulin, respectively, in the presence or in the absence of 1 μM rosiglitazone.

Fluorescence microscopy analysis

Cells were cultivated on 24 × 24 mm coverslips and transfected with YFP-tagged h289X, h319X, wt hATGL, or YFP control and CFP-tagged mG0S2 or CFP control. To induce lipid-droplet formation, cells were incubated in the presence of 0.4 mM oleic acid complexed to essentially FA-free BSA in a molar ratio of 3:1 for 20 h. For microscopy, coverslips were mounted on standard microscope slides and analyzed using a Leica SP2 confocal microscope (Leica Microsystems, Mannheim, Germany) with spectral detection and a 100× oil immersion objective (NA 1.4). CFP and YFP fluorescence were excited at 458 and 514 nm, respectively, and detected in the range between 477 and 535 nm. Nucleic acid staining was performed using Hoechst 34580 reagent (Life Technologies). Hoechst fluorescence was excited at 405 nm and detected in the range between 420 and 450 nm.

Determination of protein concentrations

Protein concentrations were determined using Bio-Rad protein assay according to the manufacturer's protocol (Bio-Rad 785, Bio-Rad Laboratories, Munich, Germany), using BSA as standard. Alternatively, protein measurements were performed using the BCA reagent (Pierce, Rockford, IL).

Statistical analysis

Statistical analyses were determined by Student unpaired *t*-test (two tailed). The levels of statistical significance were $*P < 0.05$, $**P < 0.01$, and $***P < 0.001$.

RESULTS

G0S2 is expressed in murine and human adipose tissue

We first investigated the expression levels of G0S2 in various human and, for comparison, murine tissues. G0S2 protein was detectable in human and murine white adipose tissues (WAT), but it was not detectable in human and murine liver, muscle, lung, or in human brain (**Fig. 1A**).

ATGL and G0S2 but not CGI-58 expression is induced by rosiglitazone during SGBS cell differentiation

We compared the expression profiles of ATGL, CGI-58, and G0S2 during differentiation of human SGBS adipocytes. Western blotting analyses revealed that ATGL and G0S2 expression levels increased during differentiation of SGBS cells, with highest protein expression at day 8 (Fig. 1B, left panels). Upon removal of rosiglitazone from the differentiation medium (at day 8), expression levels of ATGL and G0S2 markedly decreased. When rosiglitazone remained in the media (Fig. 1B, right panels) expression levels of ATGL and G0S2 remained much higher. In contrast, CGI-58 protein expression was constant between days 1 and 14 of differentiation, irrespective of rosiglitazone (Fig. 1B, left and right panels). For comparison, we differentiated murine 3T3-L1 adipocytes in the presence or absence of rosiglitazone and analyzed ATGL, CGI-58, and G0S2 expression. As observed for human SGBS adipocytes, in murine 3T3-L1 adipocytes, ATGL and tentatively also G0S2 expression was induced by rosiglitazone, which was not observed for CGI-58 protein expression (compare left and right panels of Fig. 1C). This indicates that expression of ATGL and G0S2, but not of CGI-58, is induced during differentiation of human and murine adipocytes by the peroxisome proliferator-activated receptor-γ (PPAR-γ) activator rosiglitazone.

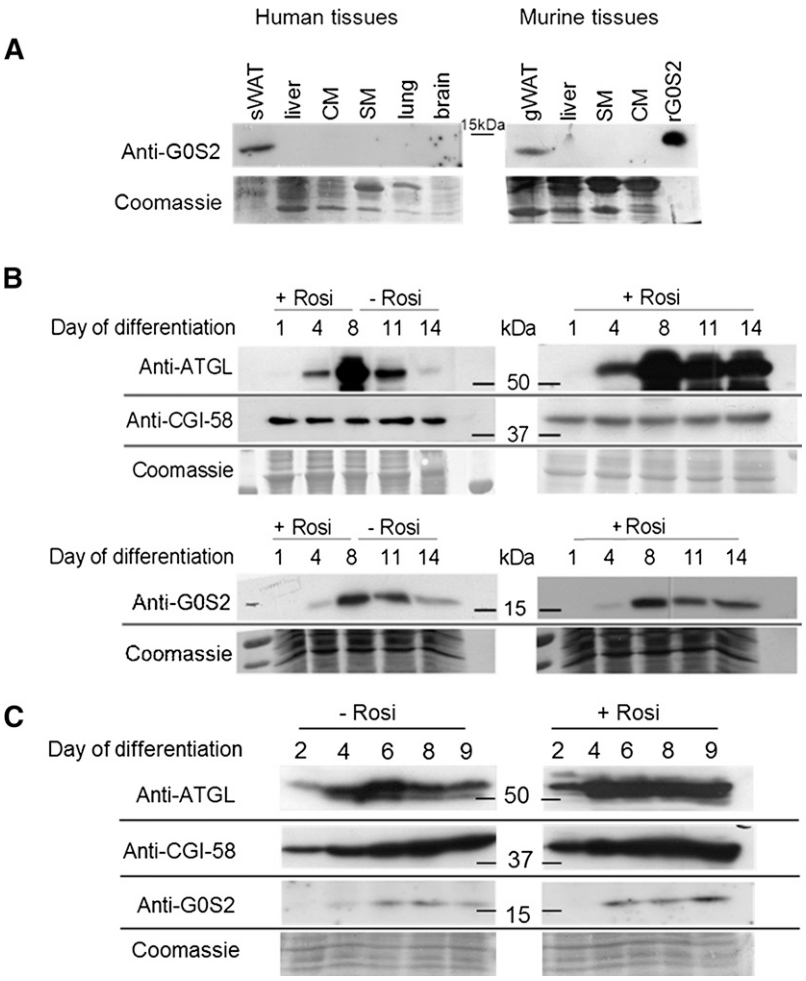

Fig. 1. (A) G0S2 is expressed in human and murine adipose tissue. Human and murine tissue extracts (50 μg protein of 20,000 *g* infranatant) and, as a control, Cos-7 lysate-containing recombinant His-tagged hG0S2 (20 μg protein) were analyzed by Western blotting. G0S2 was detected using a purified polyclonal antibody directed against a human and murine peptide. As loading control, membranes were stained with Coomassie blue. (B, C) ATGL and G0S2 but not CGI-58 expression is induced by rosiglitazone during SGBS (B) and 3T3-L1 (C) differentiation. SGBS cells were differentiated for 8 days. Then, rosiglitazone was either omitted from the differentiation media or kept until day 14. 3T3-L1 cells were differentiated for 9 days either in the presence or absence of rosiglitazone. At various times, cells were harvested and lysates (75 μg protein) analyzed for ATGL, G0S2, and CGI-58 expression by Western blot analyses using antibodies specific for ATGL, CGI-58, and G0S2. As loading control, membranes were stained with Coomassie blue. CM, cardiac muscle; gWAT, gonadal white adipose tissue; rG0S2, Cos-7 lysate-containing recombinant human G0S2; Rosi, rosiglitazone; SM, skeletal muscle; sWAT, subcutaneous white adipose tissue.

Human ATGL and adipose tissue lipolysis are inhibited by G0S2

To investigate the inhibitory effect of G0S2 on ATGL activity, we expressed human His-tagged proteins in Cos-7 cells and prepared lysates for in vitro TG hydrolase activity assays (**Fig. 2A**, inset). As depicted in Fig. 2A, increasing amounts of hG0S2 dose-dependently inhibited hCGI-58-stimulated hATGL activity. Half-maximal inhibition was achieved at ~0.4 mol hG0S2 per mol hATGL. hG0S2 reduced the activity of hATGL to a similar degree (~70%) in the presence or absence of CGI-58 (Fig. 2B). To investigate whether also human adipose tissue lipolysis is inhibited by G0S2, we measured TG hydrolase activity of human subcutaneous adipose tissue extracts in the absence or presence of purified recombinant hG0S2 (Fig. 2C, D). Addition of purified hG0S2 reduced TG hydrolase activity by ~35%, indicating that G0S2 inhibits also human adipose tissue lipolysis, presumably through inhibition of ATGL activity (Fig. 2C).

G0S2 affects activity and localization of C-terminally truncated human ATGL variants

C-terminally truncated human ATGL variants associated with the development of NLSDM exhibit increased in vitro TG hydrolase activity but do not bind to cellular LDs due to the loss of the C-terminal lipid binding region (21). To test whether the lack of the C-terminus affects G0S2-mediated inhibition of ATGL, we overexpressed these mutant variants in Cos-7 cells and measured their activity in the presence of hCGI-58 with or without addition of hG0S2. In accordance with previous data (21), truncated variants h289X and h319X exhibited increased in vitro activity compared with hATGL. The addition of hG0S2 led to complete inhibition of wild-type and mutant enzymes, implicating that G0S2 inhibits ATGL activity independent of the C-terminal part of the enzyme (**Fig. 3A**). Next, we investigated the effect of G0S2 on the localization of ATGL variants by confocal laser-scanning live cell imaging. For that purpose, we expressed YFP-tagged full length and C-terminally truncated ATGL (h289X and h319X) in Cos-7 cells. In accordance with previous findings, hATGL localized to LDs, whereas truncated ATGL variants appeared in the cytosol. Coexpression of CFP-tagged G0S2 did not affect the localization of hATGL. Interestingly, however, coexpression of C-terminally truncated YFP-tagged ATGL variants with CFP-tagged G0S2 led to a translocation of ATGL mutants to the surface of LDs (Fig. 3B). This suggests that G0S2 can anchor ATGL to the LD independent of its C-terminal lipid binding region. In control experiments, coexpression of neither CFP-tagged G0S2 with YFP nor of YFP-tagged ATGL with CFP affected localization of the coexpressed proteins.

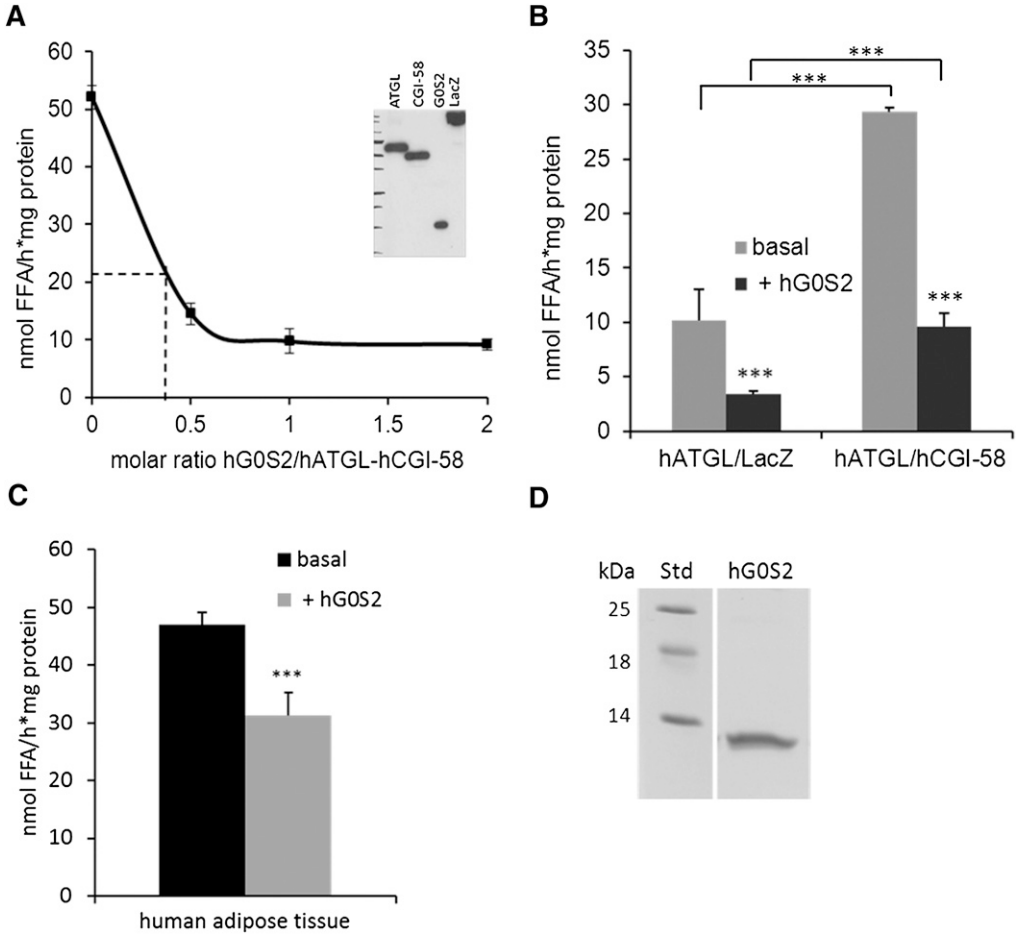

Fig. 2. Human ATGL is inhibited by G0S2. (A) Cos-7 cell lysates containing hATGL and hCGI-58 (both His-tagged) were mixed at equimolar ratio and then increasing amounts of lysates containing hG0S2 (His-tagged) or, as a control, β-galactosidase (LacZ, His-tagged) were added. Then, in vitro TG hydrolase activities were determined. As substrate, ^{3}H-triolein emulsified with PC:PI was added and incubated for 1 h at 37°C. FFAs were extracted and radioactivity measured by liquid scintillation counting. (A, inset). Expression levels of recombinant proteins were assessed by Western blotting using anti-His antibody and quantified by densitometric analysis. Quantified expression levels were used for calculating equimolar ratios. (B) Cell lysates containing hATGL were mixed with lysates containing hCGI-58 at equimolar ratio and, as a control, LacZ. Then, to one-half of the mixtures, hG0S2-containing lysates at equimolar ratios were added and in vitro TG hydrolase activities were determined. Molar ratios of recombinant proteins were determined as in (A) inset. (C) Human adipose tissue TG hydrolase activity is inhibited by hG0S2. In vitro TG hydrolase activity of human subcutaneous adipose tissue was determined in the absence or presence of purified hG0S2 as in (A). Data are mean ± SD of n = 3 and representative of two independent experiments (***$P < 0.001$). (D) Purity of hG0S2 (5 μg) was assessed by SDS-PAGE (12.5%) using a prestained protein standard (Std, Bio-Rad Laboratories, UK).

ATGL and HSL are the major lipolytic enzymes in human SGBS adipocytes

We have previously shown that the combined lack of ATGL and HSL activity leads to an almost complete loss of hormone-stimulated lipolysis in murine adipose tissue (23). Next, we explored the relative contribution of these enzymes to lipolysis of human SGBS adipocytes. For this, we employed shRNA-mediated silencing of ATGL expression using an adenovirus encoding shRNA for ATGL, which yielded ~75% knockdown of ATGL expression (shATGL, **Fig. 4E**). Then we determined lipolysis of ATGL silenced and control SGBS adipocytes in the absence and presence of HSL-specific inhibitor 76-0079 (23). Inhibition of HSL led to a ~60% and ~77% decrease in FFA release under basal and forskolin-stimulated conditions, respectively (Fig. 4A, B). Silencing of ATGL led to ~75% and ~72% reduction in FFA release under basal (Fig. 4A) and forskolin-stimulated conditions (Fig. 4B), respectively. Inhibition of both ATGL and HSL activity resulted in ~97% and ~91% reduction in FFA release under basal and stimulated conditions, respectively (Fig. 4A, B).

In accordance with reduced FFA release, intracellular TG levels were elevated ~1.9-fold in ATGL-silenced adipocytes. Addition of the HSL-specific inhibitor to the ATGL-silenced adipocytes did not significantly affect intracellular TG levels (Fig. 4C). However, inhibition of HSL in SGBS adipocytes led to massive diacylglycerol (DG) accumulation (~4.5-fold compared with control), verifying the important role of HSL in DG-catabolism (Fig. 4D). Together, the results indicate that ATGL is rate-limiting for TG hydrolysis and HSL for DG hydrolysis in human adipocytes.

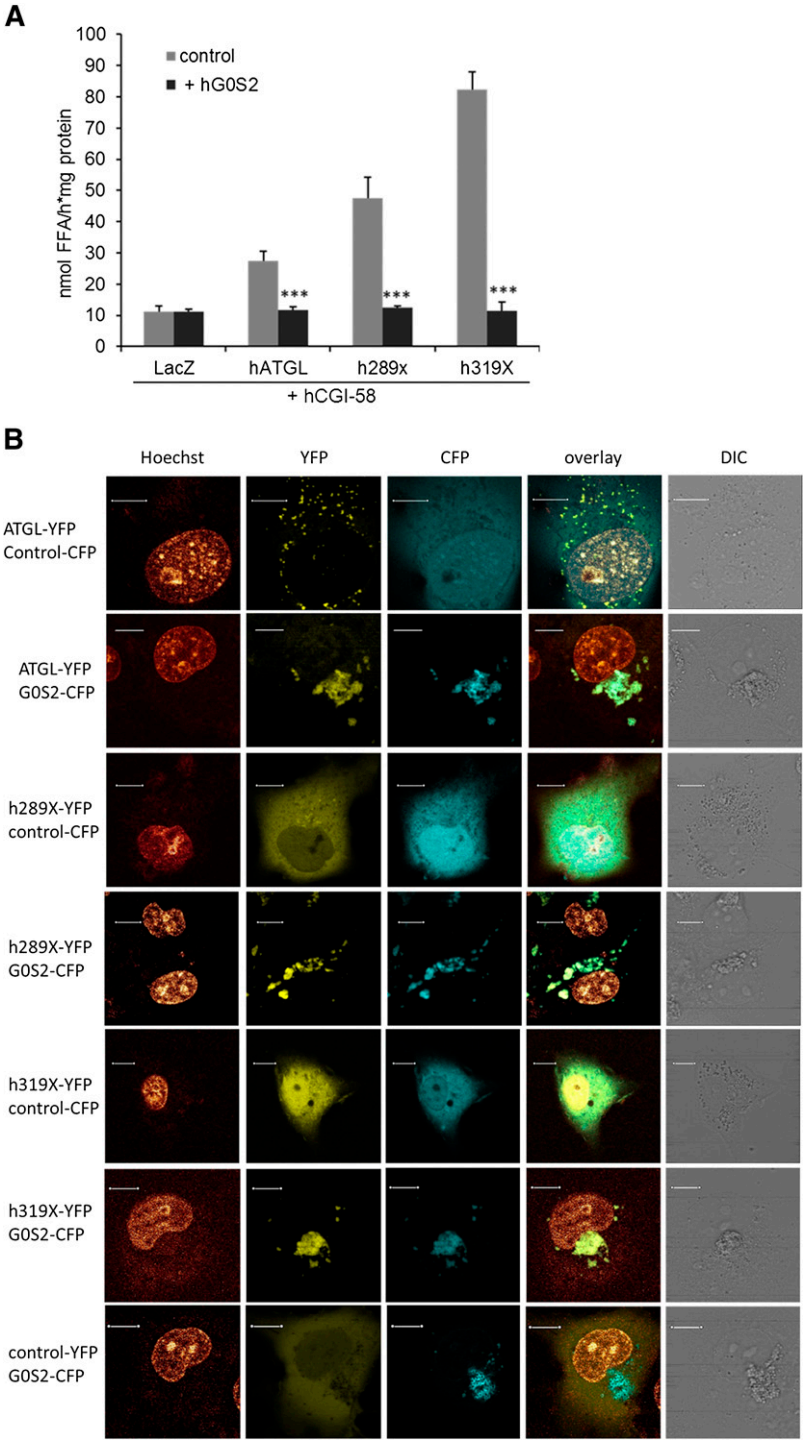

Fig. 3. (A) C-terminally truncated human ATGL mutants, which are known to cause NLSDM, are inhibited by G0S2. Cos-7 cell lysates containing full-length hATGL or C-terminally truncated variants 289X (h289X), or 319X (h319X) were mixed with lysates containing hCGI-58. Then lysates containing either hG0S2 or, as control, LacZ were added and in vitro TG hydrolase activity was determined. As substrate, ^{3}H-triolein emulsified with PC:PI was added and incubated for 1 h at 37°C. FFAs were extracted and radioactivity measured by liquid scintillation counting. Data are mean + SD of n = 3 and representative of three independent experiments (***$P < 0.001$). (B) G0S2 directs C-terminally truncated ATGL mutants to the LDs. Cos-7 cells were transfected with YFP-tagged hATGL, h289X, h319X, or YFP control and CFP-tagged mG0S2 or CFP-control. To induce LD formation, cells were incubated with 0.4 mM oleic acid. Localization of fluorescent-tagged hATGL, truncated variants, and G0S2 was determined by laser-scanning live cell imaging. Counterstaining of the nucleus was performed by nucleic acid staining using Hoechst 34580 reagent. DIC, differential interference contrast. Bars indicate 3 μm.

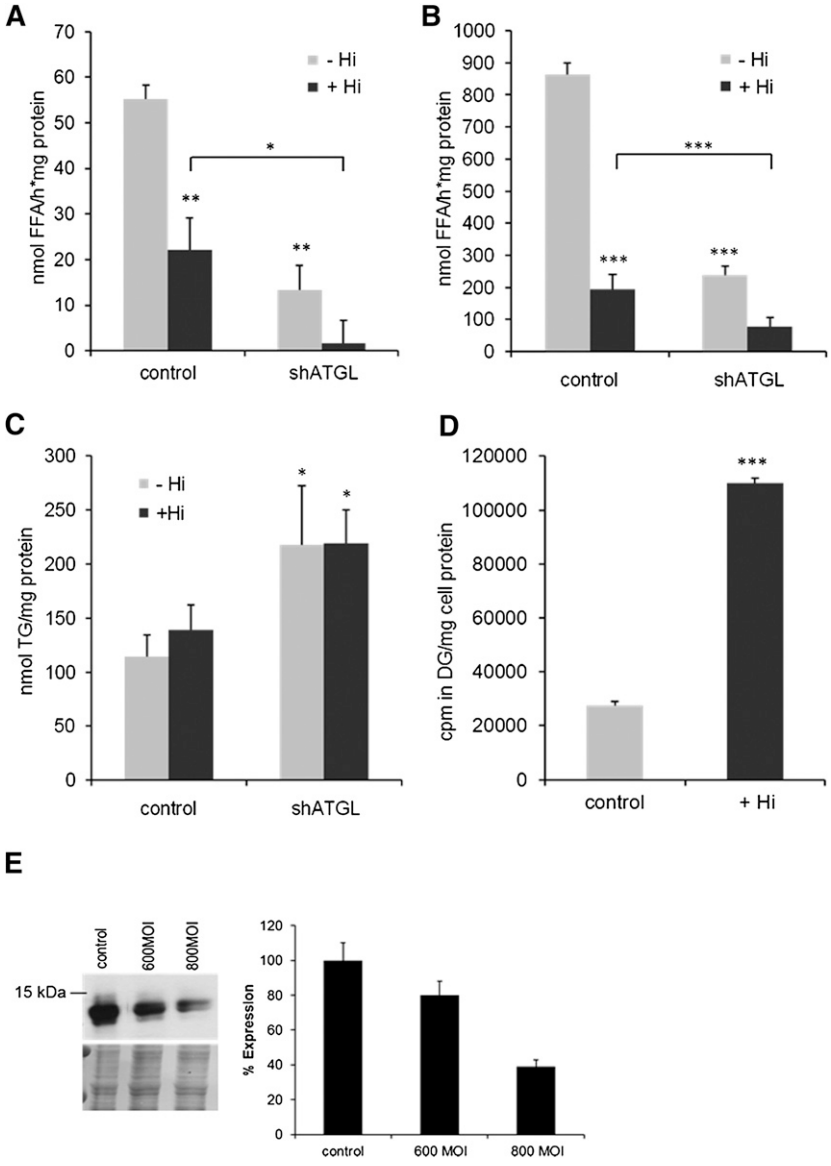

Fig. 4. Silencing of ATGL expression in human SGBS cells leads to reduced lipolysis and enhanced TG accumulation. Differentiated SGBS adipocytes were infected with different MOI of adenoviruses encoding shRNA specific for hATGL (shATGL) or LacZ (control). (A, B) Forty-eight hours after infection, cells were incubated in DMEM containing 2% BSA (FA free) in the presence or absence of a HSL-specific inhibitor (Hi) for 60 min. Then, media were replaced and cells incubated for 120 min in the absence (A) or presence (B) of 10 μM forskolin, and the release of FFAs into media was determined. (C) Total lipids of cells were extracted, dried, and redissolved in Triton X-100, and TG content was determined enzymatically. (D) Differentiated SGBS cells were loaded with 0.4 mM oleic acid and 4 mCi ^{3}H-9,10-oleate/mmol as tracer (1 μCi per 6-well). Then cells were washed and incubated in medium containing 2% BSA (FA free) in the presence or absence of Hi. After 60 min, media were replaced by identical fresh media containing 10 μM forskolin in the presence or absence of Hi. After 120 min, total lipids were extracted and separated by TLC. Bands corresponding to DG were excised and radioactivity determined by liquid scintillation counting. Data are mean + SD of n = 4 and are representative of three independent experiments (*$P < 0.05$; **$P < 0.01$; ***$P < 0.001$). (E) The efficiency of shRNA-mediated silencing of hATGL using two different MOI was assessed by Western blot analysis using an ATGL-specific antibody. Coomassie blue staining was used as a loading control.

G0S2 regulates lipolysis in human SGBS adipocytes

To explore the effect of G0S2 on human lipolysis, we overexpressed G0S2 using adenovirus (adG0S2) in SGBS adipocytes (~1.8-fold overexpression at 800 MOI, **Fig. 5B**) and determined forskolin-stimulated FFA release in the presence and absence of HSL inhibitor. G0S2 overexpression resulted in a decrease in FFA release by ~55% (Fig. 5A, B). Addition of the HSL inhibitor to control cells reduced forskolin-stimulated FFA release by ~60%. Notably, the adenoviral overexpression of G0S2 in presence of the HSL inhibitor led to almost complete ablation (~97%) of FFA release (Fig. 5A). Similar results were obtained using the shATGL construct and the HSL inhibitor (compare Fig. 5A with Fig. 4B). Finally, to investigate the impact of endogenous G0S2 on lipolysis in

SGBS adipocytes, we electroporated cells with siRNA directed against G0S2 (siG0S2) to silence endogenous G0S2 expression, which yielded in about 70% silencing (Fig. 5C). Because of the lower cell numbers used for siRNA transfection experiments, we labeled cells with ^{3}H-oleic acid and measured ^{3}H-FFA release. G0S2 silencing led to∼1.8-fold increase in forskolin-stimulated FFA release (Fig. 5D), demonstrating an important role of endogenously expressed G0S2 in the regulation of human lipolysis.

DISCUSSION

An imbalance in the synthesis and degradation of intracellular lipids can result in either lipodystrophy or obesity. Both conditions are linked to the development of diseases, such as type 2 diabetes (24), hepatic steatosis (25), cardiovascular diseases (26), and certain types of cancer (27, 28). Accordingly, it is indispensable to understand the principle mechanisms underlying the storage and usage of body fat. In mice, it has been shown that ATGL is the rate-limiting enzyme in lipolysis and that two proteins, CGI-58 and G0S2, directly affect ATGL activity in an antipodal manner (8, 13). CGI-58 activates and G0S2 inhibits ATGL activity in vitro and in cultured murine cells. Our study aimed to elucidate the role of G0S2 in human lipolysis. We show that G0S2 efficiently inhibits human ATGL in vitro and strongly affects lipolysis in human adipocytes. Thus, dysregulation of this protein could affect lipolysis and may represent one of the causative factors leading to aberrant lipolysis in metabolic diseases.

The role of ATGL and HSL in human lipolysis is still a matter of debate. Bezaire et al. (29) studied TG mobilization in differentiated human adipose-derived stem (hMADS) cells with silencing or overexpressing ATGL and HSL. In their study, they found that ATGL is rate-limiting

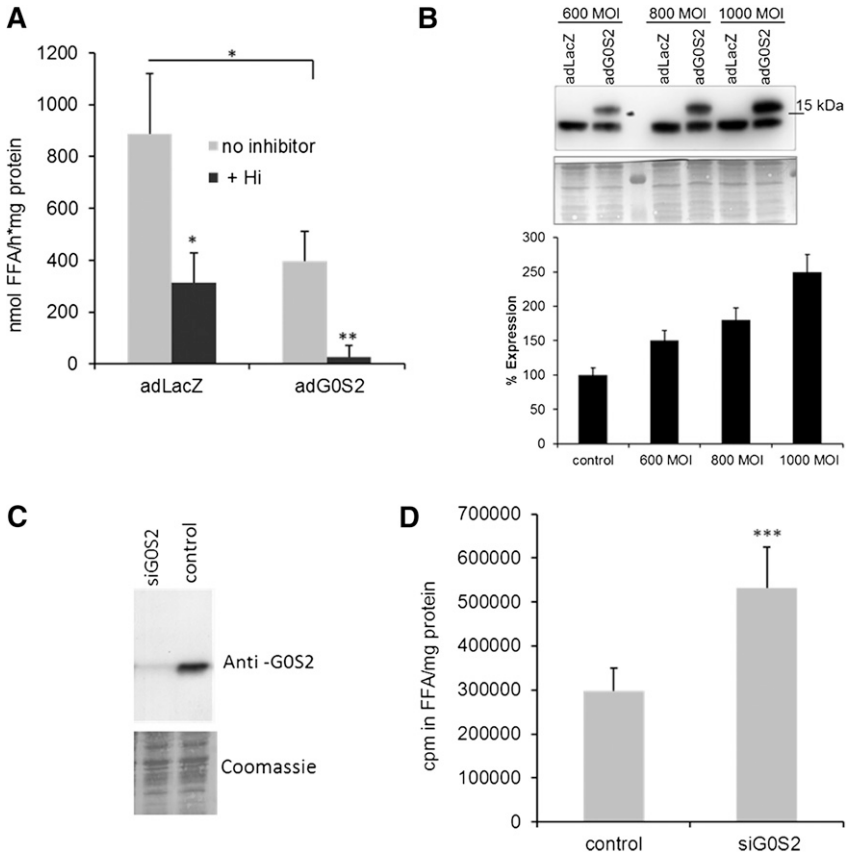

Fig. 5. Lipolysis of human SGBS adipocytes is inhibited by G0S2. (A) Differentiated SGBS adipocytes were infected with adenoviruses (1,000 MOI) encoding G0S2 (adG0S2) and, as control, LacZ (adlacZ). After 48 h of infection, cells were incubated with 25 μM of a HSL-specific inhibitor (Hi) or solvent DMSO for 60 min. Then cells were incubated with media containing 2% BSA (FA free), 10 μM forskolin, and without or with 25 μM Hi for 120 min. FFA release into supernatant was determined. (B) Overexpression of G0S2 (600, 800, and 1000 MOI) was assessed by Western blotting analysis (C) Differentiated SGBS adipocytes were electroporated with siRNA specific for hG0S2 (siG0S2) or control siRNA. Silencing of G0S2 expression was assessed by Western blotting using a G0S2-specific antibody. Coomassie blue staining was used as loading control. (D) Differentiated SGBS adipocytes were electroporated with siG0S2 or control siRNA. Thereafter, cells were loaded with 0.4 mM oleic acid (complexed to FA-free BSA) and 4 mCi ^{3}H-9,10-oleate/mmol as tracer (1 μCi per 6-well). Then cells were washed and incubated for 60 min in media containing 2% BSA (FA free) and 10 μM forskolin. Radioactivity in the supernatant was determined by liquid scintillation counting. Data are mean + SD of n = 4 and are representative of two independent experiments (*$P < 0.05$; **$P < 0.01$; ***$P < 0.001$).

for lipolysis under basal and hormone-stimulated conditions. In another study, Ryden et al. (30) performed similar experiments using RNAi technology but employing human mesenchymal stem cell (hMSC) adipocytes. The conclusion of this study was that ATGL plays a role in basal but not in stimulated lipolysis, which is primarily dependent on HSL activity. In our study, we used SGBS cells as a model for human adipocyte lipolysis. SGBS cells derive from the subcutaneous adipose tissue of a patient suffering from Simpson-Golabi-Behmel syndrome, a rare congenital overgrowth disease. These cells were shown to possess a high capacity for adipocyte differentiation (31–33). Furthermore, studies on the expression of adipocyte-specific genes, as well as on lipogenesis and lipolysis, demonstrated that differentiated SGBS adipocytes do not differ from primary human adipocytes (34). Our studies support the observations of Bezaire et al. that ATGL is required for efficient lipolysis in the basal and stimulated state. Inhibition of ATGL led to an accumulation of TG, whereas inhibition of HSL led to the accumulation of DG, suggesting a rate-limiting role of ATGL in TG and HSL in DG hydrolysis in human adipocytes, similar to that previously observed in murine adipose tissue (23). Furthermore, we found that overexpression of G0S2 in the presence of the HSL inhibitor almost completely abolished lipolysis. These results corroborate that ATGL and HSL are the major lipases in human adipocyte lipolysis and act in concert to mobilize stored TG. Furthermore, using subcutaneous WAT samples of human subjects, we demonstrate that G0S2 inhibits lipolysis of human WAT lysates similar to that observed in SGBS adipocytes.

During human and murine adipocyte differentiation, we observed that G0S2 expression was concomitantly upregulated with ATGL. The expression of both proteins was strongly dependent on the presence of the PPAR-γ agonist rosiglitazone, confirming previous reports identifying ATGL and G0S2 as PPAR-γ targets (13, 19, 35, 36). In contrast, expression levels of CGI-58 remained unaffected by rosiglitazone treatment. Importantly, G0S2, but not CGI-58, expression is downregulated by β-adrenergic stimulation and fasting and upregulated by refeeding and insulin (8, 17). These findings suggest that these two proteins are controlled by different hormonal pathways. Apparently, CGI-58 function is primarily controlled on the posttranslational level. In the basal state, CGI-58 is bound to perilipin-1 and not available for ATGL activation. In response to β-adrenergic stimulation, protein kinase A phosphorylates perilipin-1, leading to the liberation of CGI-58, which then activates ATGL (37, 38). Perilipin-5 (OXPAT) also has been shown to interact with ATGL (39). Although the expression level of perilipin-5 in WAT is very low, it might well be that it also participates in the regulation of ATGL activity and/or translocation (40). To date, it is unknown whether perilipin-5 and G0S2 compete for binding ATGL. Lu et al. (41) reported that G0S2 and CGI-58 do not compete for ATGL binding as G0S2 is able to bind to ATGL in the absence or presence of CGI-58. Our data confirm these observations, showing that G0S2 efficiently inhibits human ATGL activity in the presence or absence of CGI-58. Notably, G0S2 anchors C-terminally truncated ATGL mutants to LDs. These mutant variants of ATGL cause NLSDM and are known to be defective in LD localization. Our observations suggest that not only ATGL activity but also LD binding of the enzyme is influenced by G0S2. Interestingly, ATGL and G0S2 have been shown to colocalize at the LD during basal and hormone-stimulated lipolysis (13). These observations imply that the G0S2-mediated inhibition of ATGL activity cannot be reversed simply by the binding of CGI-58 to the ATGL:G0S2 protein complex. Given that G0S2 and ATGL interact on the LD surface in lipolytic-stimulated adipocytes, it is reasonable to assume that additional regulatory events must exist, enabling ATGL to hydrolyze TG. These regulatory events may include posttranslational modification of either ATGL or G0S2. So far, G0S2 has not been reported to be modified by phosphorylation or other protein modifications. Conversely, ATGL has been shown to be phosphorylated (42) and moreover, ATGL phosphorylation at Ser406 enhances its TG hydrolase activity (43). Thus, it is reasonable to assume that additional uncharacterized regulatory mechanisms exist that regulate the G0S2-mediated inhibition of ATGL activity.

In summary, our data demonstrate that G0S2 inhibits human ATGL activity and lipolysis of human adipose tissue and human adipocytes. The finding that G0S2 mRNA and protein expression is reduced in adipose tissue of type 2 diabetic humans suggests that enhanced ATGL activity may contribute to elevated lipolysis and plasma FA levels in type 2 diabetic patients (20). Considering the nutritional and hormonal regulation of G0S2, downregulation of this protein could represent one of the underlying mechanisms causing increased lipolysis in the insulin-resistant state.

The authors thank Sabrina Huetter and Jasmin Paar of the Institute of Molecular Biosciences, University of Graz, for excellent technical assistance. The authors thank Dr. Heimo Wolinski of the Institute of Molecular Biosciences, University of Graz, for his assistance in using laser-scanning microscopy.

REFERENCES

1. Villena, J. A., S. Roy, E. Sarkadi-Nagy, K. H. Kim, and H. S. Sul. 2004. Desnutrin, an adipocyte gene encoding a novel patatin domain-containing protein, is induced by fasting and glucocorticoids: ectopic expression of desnutrin increases triglyceride hydrolysis. *J. Biol. Chem.* **279:** 47066–47075.
2. Jenkins, C. M., D. J. Mancuso, W. Yan, H. F. Sims, B. Gibson, and R. W. Gross. 2004. Identification, cloning, expression, and purification of three novel human calcium-independent phospholipase A2 family members possessing triacylglycerol lipase and acylglycerol transacylase activities. *J. Biol. Chem.* **279:** 48968–48975.
3. Zimmermann, R., J. G. Strauss, G. Haemmerle, G. Schoiswohl, R. Birner-Gruenberger, M. Riederer, A. Lass, G. Neuberger, F. Eisenhaber, A. Hermetter, et al. 2004. Fat mobilization in adipose tissue is promoted by adipose triglyceride lipase. *Science.* **306:** 1383–1386.
4. Haemmerle, G., R. Zimmermann, M. Hayn, C. Theussl, G. Waeg, E. Wagner, W. Sattler, T. M. Magin, E. F. Wagner, and R. Zechner. 2002. Hormone-sensitive lipase deficiency in mice causes diglyceride accumulation in adipose tissue, muscle, and testis. *J. Biol. Chem.* **277:** 4806–4815.

5. Taschler, U., F. P. Radner, C. Heier, R. Schreiber, M. Schweiger, G. Schoiswohl, K. Preiss-Landl, D. Jaeger, B. Reiter, H. C. Koefeler, et al. 2011. Monoglyceride lipase deficiency in mice impairs lipolysis and attenuates diet-induced insulin resistance. *J. Biol. Chem.* **286:** 17467–17477.
6. Haemmerle, G., A. Lass, R. Zimmermann, G. Gorkiewicz, C. Meyer, J. Rozman, G. Heldmaier, R. Maier, C. Theussl, S. Eder, et al. 2006. Defective lipolysis and altered energy metabolism in mice lacking adipose triglyceride lipase. *Science.* **312:** 734–737.
7. Fischer, J., C. Lefevre, E. Morava, J. M. Mussini, P. Laforet, A. Negre-Salvayre, M. Lathrop, and R. Salvayre. 2007. The gene encoding adipose triglyceride lipase (PNPLA2) is mutated in neutral lipid storage disease with myopathy. *Nat. Genet.* **39:** 28–30.
8. Lass, A., R. Zimmermann, G. Haemmerle, M. Riederer, G. Schoiswohl, M. Schweiger, P. Kienesberger, J. G. Strauss, G. Gorkiewicz, and R. Zechner. 2006. Adipose triglyceride lipase-mediated lipolysis of cellular fat stores is activated by CGI-58 and defective in Chanarin-Dorfman syndrome. *Cell Metab.* **3:** 309–319.
9. Radner, F. P., I. E. Streith, G. Schoiswohl, M. Schweiger, M. Kumari, T. O. Eichmann, G. Rechberger, H. C. Koefeler, S. Eder, S. Schauer, et al. 2010. Growth retardation, impaired triacylglycerol catabolism, hepatic steatosis, and lethal skin barrier defect in mice lacking comparative gene identification-58 (CGI-58). *J. Biol. Chem.* **285:** 7300–7311.
10. Lefèvre, C., F. Jobard, F. Caux, B. Bouadjar, A. Karaduman, R. Heilig, H. Lakhdar, A. Wollenberg, J. L. Verret, J. Weissenbach, et al. 2001. Mutations in CGI-58, the gene encoding a new protein of the esterase/lipase/thioesterase subfamily, in Chanarin-Dorfman syndrome. *Am. J. Hum. Genet.* **69:** 1002–1012.
11. Ghosh, A. K., G. Ramakrishnan, C. Chandramohan, and R. Rajasekharan. 2008. CGI-58, the causative gene for Chanarin-Dorfman syndrome, mediates acylation of lysophosphatidic acid. *J. Biol. Chem.* **283:** 24525–24533.
12. Montero-Moran, G., J. M. Caviglia, D. McMahon, A. Rothenberg, V. Subramanian, Z. Xu, S. Lara-Gonzalez, J. Storch, G. M. Carman, and D. L. Brasaemle. 2010. CGI-58/ABHD5 is a coenzyme A-dependent lysophosphatidic acid acyltransferase. *J. Lipid Res.* **51:** 709–719.
13. Yang, X., X. Lu, M. Lombes, G. B. Rha, Y. I. Chi, T. M. Guerin, E. J. Smart, and J. Liu. 2010. The G(0)/G(1) switch gene 2 regulates adipose lipolysis through association with adipose triglyceride lipase. *Cell Metab.* **11:** 194–205.
14. Russell, L., and D. R. Forsdyke. 1991. A human putative lymphocyte G0/G1 switch gene containing a CpG-rich island encodes a small basic protein with the potential to be phosphorylated. *DNA Cell Biol.* **10:** 581–591.
15. Yamada, T., C. S. Park, A. Burns, D. Nakada, and H. D. Lacorazza. 2012. The cytosolic protein G0S2 maintains quiescence in hematopoietic stem cells. *PLoS ONE.* **7:** e38280.
16. Welch, C., M. K. Santra, W. El-Assaad, X. Zhu, W. E. Huber, R. A. Keys, J. G. Teodoro, and M. R. Green. 2009. Identification of a protein, G0S2, that lacks Bcl-2 homology domains and interacts with and antagonizes Bcl-2. *Cancer Res.* **69:** 6782–6789.
17. Nielsen, T. S., M. H. Vendelbo, N. Jessen, S. B. Pedersen, J. O. Jorgensen, S. Lund, and N. Moller. 2011. Fasting, but not exercise, increases adipose triglyceride lipase (ATGL) protein and reduces G(0)/G(1) switch gene 2 (G0S2) protein and mRNA content in human adipose tissue. *J. Clin. Endocrinol. Metab.* **96:** E1293–E1297.
18. Oh, S. A., Y. Suh, M. G. Pang, and K. Lee. 2011. Cloning of avian G(0)/G(1) switch gene 2 genes and developmental and nutritional regulation of G(0)/G(1) switch gene 2 in chicken adipose tissue. *J. Anim. Sci.* **89:** 367–375.
19. Yang, X., X. Zhang, B. L. Heckmann, X. Lu, and J. Liu. 2011. Relative contribution of adipose triglyceride lipase and hormone-sensitive lipase to tumor necrosis factor-alpha (TNF-alpha)-induced lipolysis in adipocytes. *J. Biol. Chem.* **286:** 40477–40485.
20. Nielsen, T. S., U. Kampmann, R. R. Nielsen, N. Jessen, L. Orskov, S. B. Pedersen, J. O. Jørgensen, S. Lund, and N. Møller. 2012. Reduced mRNA and protein expression of Perilipin A and G0/G1 switch gene 2 (G0S2) in human adipose tissue in poorly controlled type 2 diabetes. *J. Clin. Endocrinol. Metab.* **97:** E1348–E1352.
21. Schweiger, M., G. Schoiswohl, A. Lass, F. P. Radner, G. Haemmerle, R. Malli, W. Graier, I. Cornaciu, M. Oberer, R. Salvayre, et al. 2008. The C-terminal region of human adipose triglyceride lipase affects enzyme activity and lipid droplet binding. *J. Biol. Chem.* **283:** 17211–17220.
22. Graham, F. L., and A. J. van der Eb. 1973. A new technique for the assay of infectivity of human adenovirus 5 DNA. *Virology.* **52:** 456–467.
23. Schweiger, M., R. Schreiber, G. Haemmerle, A. Lass, C. Fledelius, P. Jacobsen, H. Tornqvist, R. Zechner, and R. Zimmermann. 2006. Adipose triglyceride lipase and hormone-sensitive lipase are the major enzymes in adipose tissue triacylglycerol catabolism. *J. Biol. Chem.* **281:** 40236–40241.
24. Stumvoll, M., B. J. Goldstein, and T. W. van Haeften. 2005. Type 2 diabetes: principles of pathogenesis and therapy. *Lancet.* **365:** 1333–1346.
25. Marchesini, G., M. Brizi, G. Bianchi, S. Tomassetti, E. Bugianesi, M. Lenzi, A. J. McCullough, S. Natale, G. Forlani, and N. Melchionda. 2001. Nonalcoholic fatty liver disease: a feature of the metabolic syndrome. *Diabetes.* **50:** 1844–1850.
26. Björntorp, P. 1990. "Portal" adipose tissue as a generator of risk factors for cardiovascular disease and diabetes. *Arteriosclerosis.* **10:** 493–496.
27. Adami, H. O., J. McLaughlin, A. Ekbom, C. Berne, D. Silverman, D. Hacker, and I. Persson. 1991. Cancer risk in patients with diabetes mellitus. *Cancer Causes Control.* **2:** 307–314.
28. Strickler, H. D., J. Wylie-Rosett, T. Rohan, D. R. Hoover, S. Smoller, R. D. Burk, and H. Yu. 2001. The relation of type 2 diabetes and cancer. *Diabetes Technol. Ther.* **3:** 263–274.
29. Bezaire, V., A. Mairal, C. Ribet, C. Lefort, A. Girousse, J. Jocken, J. Laurencikiene, R. Anesia, A. M. Rodriguez, M. Ryden, et al. 2009. Contribution of adipose triglyceride lipase and hormone-sensitive lipase to lipolysis in hMADS adipocytes. *J. Biol. Chem.* **284:** 18282–18291.
30. Rydén, M., J. Jocken, V. van Harmelen, A. Dicker, J. Hoffstedt, M. Wiren, L. Blomqvist, A. Mairal, D. Langin, E. Blaak, et al. 2007. Comparative studies of the role of hormone-sensitive lipase and adipose triglyceride lipase in human fat cell lipolysis. *Am. J. Physiol. Endocrinol. Metab.* **292:** E1847–E1855.
31. Simpson, J. L., S. Landey, M. New, and J. German. 1975. A previously unrecognized X-linked syndrome of dysmorphia. *Birth Defects Orig. Artic. Ser.* **11:** 18–24.
32. Golabi, M., and L. Rosen. 1984. A new X-linked mental retardation-overgrowth syndrome. *Am. J. Med. Genet.* **17:** 345–358.
33. Behmel, A., E. Plochl, and W. Rosenkranz. 1984. A new X-linked dysplasia gigantism syndrome: identical with the Simpson dysplasia syndrome? *Hum. Genet.* **67:** 409–413.
34. Wabitsch, M., R. E. Brenner, I. Melzner, M. Braun, P. Moller, E. Heinze, K. M. Debatin, and H. Hauner. 2001. Characterization of a human preadipocyte cell strain with high capacity for adipose differentiation. *Int. J. Obes. Relat. Metab. Disord.* **25:** 8–15.
35. Zandbergen, F., S. Mandard, P. Escher, N. S. Tan, D. Patsouris, T. Jatkoe, S. Rojas-Caro, S. Madore, W. Wahli, S. Tafuri, et al. 2005. The G0/G1 switch gene 2 is a novel PPAR target gene. *Biochem. J.* **392:** 313–324.
36. Kershaw, E. E., M. Schupp, H. P. Guan, N. P. Gardner, M. A. Lazar, and J. S. Flier. 2007. PPARgamma regulates adipose triglyceride lipase in adipocytes in vitro and in vivo. *Am. J. Physiol. Endocrinol. Metab.* **293:** E1736–E1745.
37. Gandotra, S., K. Lim, A. Girousse, V. Saudek, S. O'Rahilly, and D. B. Savage. 2011. Human frame shift mutations affecting the carboxyl terminus of perilipin increase lipolysis by failing to sequester the adipose triglyceride lipase (ATGL) coactivator AB-hydrolase-containing 5 (ABHD5). *J. Biol. Chem.* **286:** 34998–35006.
38. Zechner, R., R. Zimmermann, T. O. Eichmann, S. D. Kohlwein, G. Haemmerle, A. Lass, and F. Madeo. 2012. FAT SIGNALS–lipases and lipolysis in lipid metabolism and signaling. *Cell Metab.* **15:** 279–291.
39. Granneman, J. G., H. P. Moore, E. P. Mottillo, Z. Zhu, and L. Zhou. 2011. Interactions of perilipin-5 (Plin5) with adipose triglyceride lipase. *J. Biol. Chem.* **286:** 5126–5135.
40. Wolins, N. E., B. K. Quaynor, J. R. Skinner, A. Tzekov, M. A. Croce, M. C. Gropler, V. Varma, A. Yao-Borengasser, N. Rasouli, P. A. Kern, et al. 2006. OXPAT/PAT-1 is a PPAR-induced lipid droplet protein that promotes fatty acid utilization. *Diabetes.* **55:** 3418–3428.
41. Lu, X., X. Yang, and J. Liu. 2010. Differential control of ATGL-mediated lipid droplet degradation by CGI-58 and G0S2. *Cell Cycle.* **9:** 2719–2725.
42. Bartz, R., J. K. Zehmer, M. Zhu, Y. Chen, G. Serrero, Y. Zhao, and P. Liu. 2007. Dynamic activity of lipid droplets: protein phosphorylation and GTP-mediated protein translocation. *J. Proteome Res.* **6:** 3256–3265.
43. Ahmadian, M., M. J. Abbott, T. Tang, C. S. Hudak, Y. Kim, M. Bruss, M. K. Hellerstein, H. Y. Lee, V. T. Samuel, G. I. Shulman, et al. 2011. Desnutrin/ATGL is regulated by AMPK and is required for a brown adipose phenotype. *Cell Metab.* **13:** 739–748.